Frederick P. "Ted" Schiffley, II
BWROG Chairman
Tel: (630) 657-3897
Fax: (630) 657-4328
frederick.schiffley@exeloncorp.com

c/o GE Hitachi Nuclear Energy, P.O. Box 780, 3901 Castle Hayne Road, M/C A-70, Wilmington, NC 28402 USA

BWROG-12028
June 13, 2012

Project No. 691

Document Control Desk
U.S. Nuclear Regulatory Commission
Washington, DC 20555-0001

Attention: Mr. Joe Golla (NRC)

SUBJECT: Submittal Responses to Request for Additional Information Regarding Boiling Water Reactor Owners' Group (BWROG) Licensing Topical Report BWROG-TP-11-023, Revision 0, Linear Elastic Fracture Mechanics Evaluation of General Electric Boiling Water Reactor Water Level Instrument Nozzles for Pressure-Temperature Curve Evaluations (TAC NO. ME7650)

ENCLOSURES:
1. Responses to Request for Additional Information Regarding Boiling Water Reactor Owners' Group (BWROG) Licensing Topical Report BWROG-TP-11-023, Revision 0, Linear Elastic Fracture Mechanics Evaluation of General Electric Boiling Water Reactor Water Level Instrument Nozzles for Pressure-Temperature Curve Evaluations (TAC NO. ME7650)

REFERENCES:
1. Request for Additional Information Regarding Boiling Water Reactor Owners' Group (BWROG) Licensing Topical Report BWROG-TP-11-023, Revision 0, Linear Elastic Fracture Mechanics Evaluation of General Electric Boiling Water Reactor Water Level Instrument Nozzles for Pressure-Temperature Curve Evaluations (TAC NO. ME7650)

2. BWROG-TP-11-023 (0900876.401), "Linear Elastic Fracture Mechanics Evaluation of General Electric Boiling Water Reactor Water Level Instrument Nozzles for Pressure-Temperature Curve Evaluations", Revision 0, November 2011

Dear Mr. Golla:

The BWROG is submitting for your review the enclosed responses to Request for Additional Information regarding BWROG Licensing Topical Report (LTR) BWROG-TP-11-023, Revision 0, Linear Elastic Fracture Mechanics Evaluation of General Electric Boiling Water Reactor Water Level Instrument Nozzles for Pressure-Temperature Curve Evaluations (TAC NO. ME7650).

D044
NRR

The RAI responses provided herein are associated with BWROG-TP-11-023 (0900876.401). The LTR is intended to support the BWR licensees in their development of a license amendment request to adopt Nuclear Regulatory Commission (NRC) Generic Letter (GL) 96-03. This LTR provides a bounding partial penetration style water level instrument nozzle fracture mechanics solution which can be used to obtain plant specific stress intensity factors for an internal pressure load case and a 100 °F/hr thermal ramp load case for use in developing plant specific P-T curves, without having to develop and analyze a plant specific finite element model. This LTR and the response to RAIs are non-proprietary as determined by the author.

We look forward to your timely review of the RAI responses, and to receiving a draft Safety Evaluation if there are no additional concerns. We would be happy to meet with you to discuss any issues. Should you have additional questions regarding this submittal, please contact me or Lucas Martins (BWROG – Project Manager) at (910) 819-1986.

Regards,

Frederick P. "Ted" Schiffley, II
Chairman
BWR Owners' Group

cc: C.J. Nichols, BWROG Program Manager
L. Martins, BWROG Project Manager
BWROG Primary Representatives

ENCLOSURE 1

BWROG-12028

Responses to Request for Additional Information Regarding Boiling Water Reactor Owners' Group (BWROG) Licensing Topical Report BWROG-TP-11-023, Revision 0, Linear Elastic Fracture Mechanics Evaluation of General Electric Boiling Water Reactor Water Level Instrument Nozzles for Pressure-Temperature Curve Evaluations (TAC NO. ME7650)

RAI-1

Section 2.2 of the Licensing Topical Report (LTR) BWROG-TP-11-023, Revision 0 discussed model geometry, materials, and heat transfer coefficients used in the stress analyses. The NRC staff has the following questions:

- *It is stated that, "[s]ince there is no specific material specification identified for the CS [carbon steel] nozzle inserts from Table 2-1 of Reference [13], SA-541 Class 1 is assumed." Depending on the material properties used, this assumption could change the calculated stresses significantly. Please estimate the ranges of key material properties for CS nozzle inserts and assess the impact on the LTR results and conclusion, considering that each property could be at either end of its range.*

- *It is stated that, "[t]he weld material is always assumed as Alloy 600 for the different nozzle material cases." Justify use of Alloy 600 for the variety of instrument nozzles covered by this LTR and assess the impact of this assumption on the results summarized in Figures 6-4 and 6-5 and on the conclusion presented in Section 9.0 of this LTR due to the fact that the real weld material may not be Alloy 600 material.*

- *In the thermal analysis, the heat transfer coefficient is assumed as 500 Btu/hr-ft^2-°F for the inside surface of the vessel and nozzle and 0.2 Btu/hr-ft^2-°F for the outside surface of the vessel and nozzle. Please justify the use of these coefficients in this application and cite NRC safety evaluations (SEs) accepting use of these coefficients in similar applications.*

RAI-1 Response

A. First bullet: A survey of the utility members supporting development of this LTR identified that one utility has a water level instrument nozzle fabricated from SA-508 Cl. 1 material. This is in contrast to BWRVIP-49-A [1], which was used as the initial input for this evaluation. Consequently, a thermo-elastic finite element stress analysis was performed to investigate the possible effect that Low Alloy Steel (LAS) material properties would have on the results of the fracture mechanics evaluations documented in this LTR. One

representative finite element analysis of a water level instrument nozzle configuration with LAS material properties was performed. The K_I from a 100 °F/hr cool-down transient was calculated and the difference in K_I obtained from the thermal transient for LAS and CS water level insert nozzle materials is evaluated. The modeling methodology described in the LTR was used for this evaluation; therefore, it is not documented here. Path stresses for each nozzle case were extracted over the first 1/4t path length, polynomial curve fit coefficients were calculated, and a K_{It} was determined using Eq. 2-1 of the LTR. The path length used for this study was 2.148 inches. Figure 1 shows the path stress distributions, over the first 1/4t and the polynomial curve fit equations. The results of this comparison are summarized below:

K_{IT_CS} = 21.9 ksi-in$^{0.5}$

K_{IT_LAS} = 22.7 ksi-in$^{0.5}$

Ratio = 1.037

The detailed analysis shows that the effect of the different nozzle materials is less than 4%, which is considered to be within the accuracy of the inputs and overall methodology. Recognizing that the BIE/IF solution used in the LTR has been shown in Section 7 (See Table 7-1) to be conservative by 46% for the 100 °F/hr thermal ramp load case, the minor difference (less than 4%) in the K_{It} calculated using LAS or CS material properties is not considered to be significant.

The following changes, identified in underlined text (for text addition) and ~~strikethrough~~ text (for text removal), will be made to the LTR:

Section 2.2, page 2-2, first paragraph:

The FEM includes a portion of the low alloy steel RPV shell, stainless steel RPV clad, Alloy 600 J-groove weld, Alloy 600 weld butter, nozzle insert (can be Alloy 600, Stainless Steel (SS), ~~or~~ Carbon Steel (CS) ~~per Table 2-1 of Reference~~ [13, Table 2-1], or Low Alloy Steel), Alloy 600 nozzle-to-safe end weld, and stainless steel safe end.

Table 2-2, page 2-7:

Instrument Nozzle	Alloy 600 (use N06600), Stainless Steel (use SS 304), ~~or~~ Carbon Steel, or Low Alloy Steel (use SA-541 Class 1)

Section 4.1, page 4-1, second paragraph:

The stainless steel RPV clad, Alloy 600 J-groove weld, Alloy 600 butter, Alloy 600, stainless steel, ~~or~~ carbon steel, or low alloy steel instrument nozzle, low alloy steel RPV, low alloy steel vessel pad, Alloy 600 nozzle-to-safe end weld, and stainless steel safe end are modeled as separate materials.

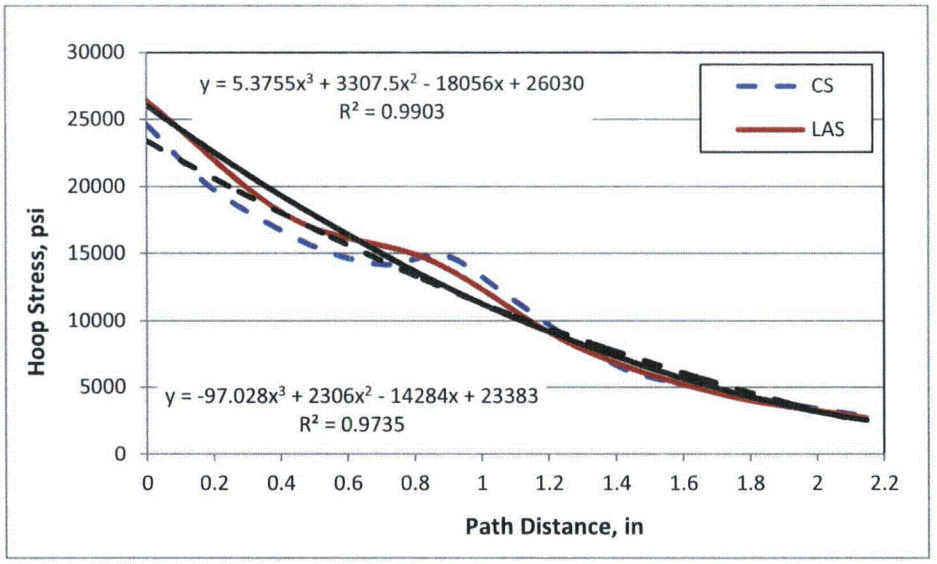

Figure 1: 1/4t path stress distributions for CS and LAS WLI nozzle FEA and polynomial curve fit equations.

B. Second bullet: All water level instrument nozzles are understood to be joined to the reactor pressure vessel (RPV) with Alloy 82/182 weld material. Since this is an inherent assumption in the evaluation, the LTR will be modified such that an additional paragraph is added to Section 1.0, Introduction, and Section 9.0, Summary, which contains the following text:

> The results of this evaluation are applicable only for plant specific water level instrument nozzle designs which fall within the bounds of those designs which were evaluated herein. Specifically, the following limitations apply:
>
> Load Cases: Internal Pressure
>
> 100 F/hr heatup/cooldown transient
>
> Geometry: See table 2-1
>
> Materials: See table 2-2

C. Third bullet: The use of 0.2 BTU/hr-ft^2-°F is the typical outside surface effective convection coefficient specified by GE for their BWR reactor pressure vessel designs. This value is used in the NRC approved in the Boiling Water Reactor Feedwater Nozzle/Sparger Final Report [3, Figure 4-132]. Since this value is the specified equivalent convection coefficient for the reflective style insulation used on the outside of the RPV this same value is used in the present analysis and is appropriate.

Considering the transient evaluated for the present evaluation, 100 °F/hr heatup/cooldown transient, the heat transfer through the RPV material and its effect on the through-wall stress distribution will be controlled by the rate of the temperature ramp rather than the convection coefficient defined for the inside surface, for convection

coefficients large enough. The value of 500 BTU/hr-ft^2-°F was selected for this analysis because:

1. It is consistent with the values typically calculated for the inside surface of the RPV; thus, is considered representative,
2. It is consistent with the range of values considered in the NRC approved Boiling Water Reactor Feedwater Nozzle/Sparger Final Report [3, Figure 4-132],
3. It is large enough that further increase in the convection coefficient has an insignificant effect on the through wall temperature distribution and maximum thermal stresses.

An evaluation performed to confirm Item 3 is summarized immediately below. A thermo-elastic analysis of a flat plate is performed using the series solution given in Reference [2]. This solution is summarized below:

$$T_{ramp}(x,t) = To + (Tf - To)\cdot\left[1 - \sum_{i=0}^{imax}\left[C_i\cdot\cos\left(\lambda_i\frac{x}{l}\right)\cdot\left[\frac{1-\exp\left[-(\lambda_i)^2\cdot Fo(t)\right]}{(\lambda_i)^2\cdot Fo(t)}\right]\right]\right] \quad (1)$$

Where: T_o is the initial wall temperature, assumed to be uniform across the thickness
T_f is the fluid temperature at time t
C_i is given by Eq. (2) below
λ_i is the i^{th} root of Eq. (3) below
x is the distance through the wall
l is the wall thickness
Fo is the Fourier number, $\alpha\, t/l^2$
α is the thermal diffusivity of the wall material
t is the time

$$C_i = \frac{4\cdot\sin(\lambda_i)}{2\cdot\lambda_i + \sin(2\cdot\lambda_i)} \quad (2)$$

$$\lambda\cdot\tan(\lambda) - Bi = 0 \quad (3)$$

Where: Bi is the Biot number, hl/k
h is the convection coefficient
l is the wall thickness
k is the thermal conductivity of the wall material

The following inputs are used:

$To := 550 \cdot \Delta°F$ Initial temperature of wall

$Tf := 70 \cdot \Delta°F$ Final fluid temperature

$h2 := 1000 \cdot \frac{BTU}{ft^2 \cdot hr \cdot \Delta°F}$ Convection coefficient at ID of wall

$h1 := 500 \cdot \frac{BTU}{ft^2 \cdot hr \cdot \Delta°F}$

$l := 6 \cdot in$ Wall thickness

$k1 := 32.3 \cdot \frac{BTU}{ft \cdot \Delta°F \cdot hr}$ Conductivity of Carbon Steel material

$E1 := 28.1 \times 10^6 \cdot \frac{lb}{in^2}$ Elastic modulus of CS material

$\varphi 1 := 6.9 \cdot 10^{-6} \cdot \frac{in}{in \cdot \Delta°F}$ Coefficient of thermal expansion of CS material

$\alpha 1 := \frac{k1}{0.283 \frac{lbm}{in^3} \cdot 0.118 \cdot \frac{BTU}{lbm \cdot \Delta°}}$ $\alpha 1 = 1.555 \times 10^{-4} \cdot \frac{ft^2}{s}$ Thermal diffusivity of CS

$\nu := 0.3$ Poisson's Ratio

$Bi\_1 := \frac{h1 \cdot l}{k1}$ $Bi\_1 = 7.7$ Biot number for first h

$Bi\_2 := \frac{h2 \cdot l}{k1}$ $Bi\_2 = 15.5$ Biot number for second h

The solution given in Eq. (1) is for the heat transfer problem of a flat plate with a convection coefficient on one side and an insulated boundary condition on the other side. The temperature distribution and through-wall temperature difference across the first 2 inches (the approximate ¼ wall thickness path length for the instrument nozzle) are shown in Figures 2 through 4 below for a h = 500 and 1000 BTU/hr-ft^2-°F. The results shown in Figures 2 through 4 show that the temperature difference across the first 1/4T of the RPV wall does not experience a significant change whether a convection coefficient of 500 BTU/hr-ft^2-°F or 1000 BTU/hr-ft^2-°F is used in the evaluation. Further increase in the convection coefficient, above 500 BTU/hr-ft^2-°F, will have no significant effect on the thermal stresses calculated for the evaluations performed in the LTR.

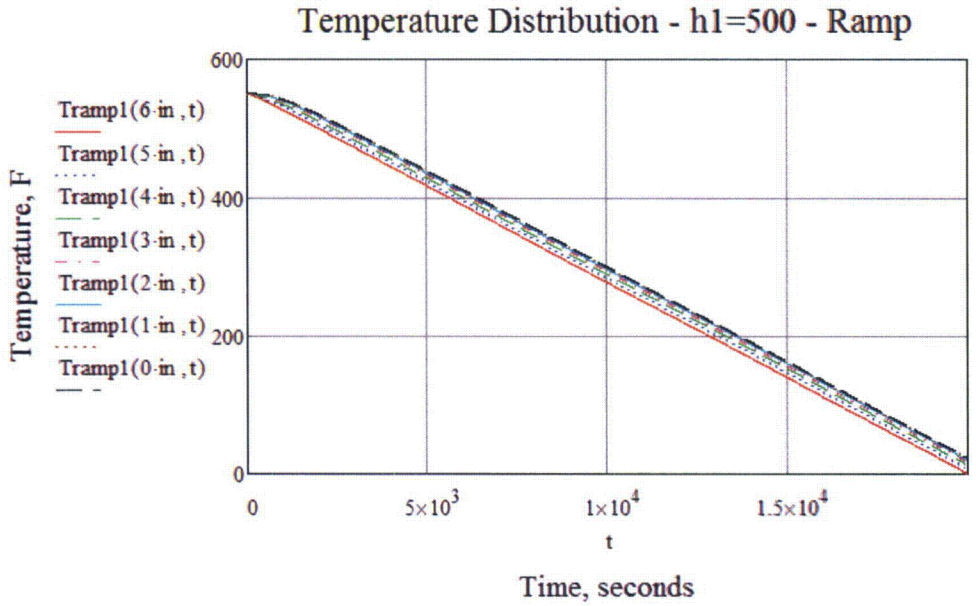

Notes:

1. x = 6 inches corresponds to the surface on which the convection coefficient of 500 BTU/hr-ft^2-˚F is applied.
2. x=0 inches corresponds to the insulated surface.
3. Ramp rate is -100 ˚F/hr.
4. For the purposes of this evaluation the ramp was not stopped at 70 ˚F; hence the continuous decrease in temperature below 70 ˚F.
5. Carbon steel material properties are used here; the results would be the same with LAS material properties.

Figure 2: Temperature distribution through the thickness of a flat plate over time, convection on one side and insulated on the other side, h=500 BTU/hr-ft^2-˚F, CS material properties, 100 ˚F/hr cool-down transient.

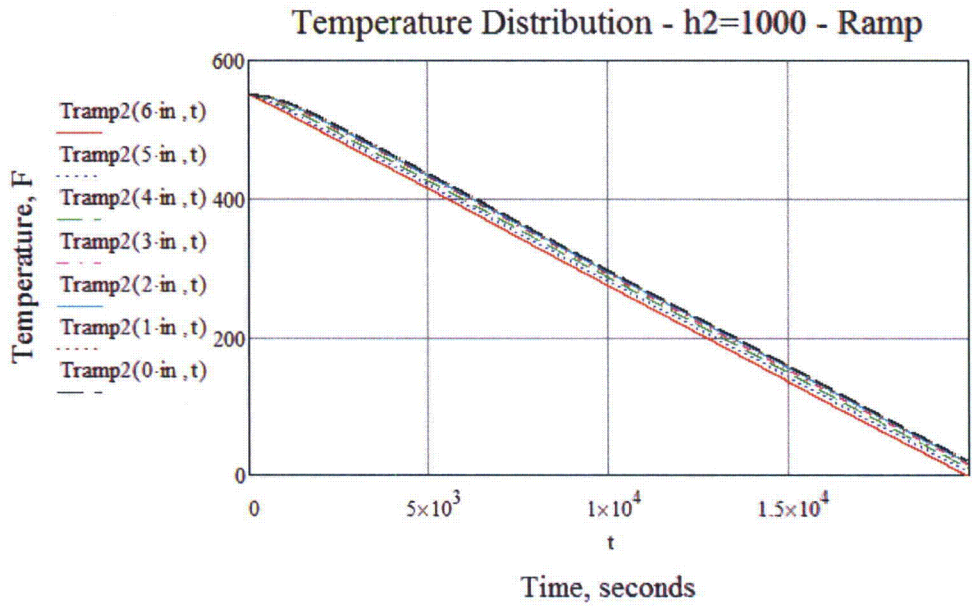

Notes:

1. x = 6 inches corresponds to the surface on which the convection coefficient of 1000 BTU/hr-ft^2-˚F is applied.
2. x=0 inches corresponds to the insulated surface.
3. Ramp rate is -100 ˚F/hr.
4. For the purposes of this evaluation the ramp was not stopped at 70 ˚F; hence the continuous decrease in temperature below 70 ˚F.
6. Carbon steel material properties are used here; the results would be the same with LAS material properties.

Figure 3: Temperature distribution through the thickness of a flat plate over time, convection on one side and insulated on the other side, h=1000 BTU/hr-ft^2-˚F, CS material properties, 100 ˚F/hr cool-down transient.

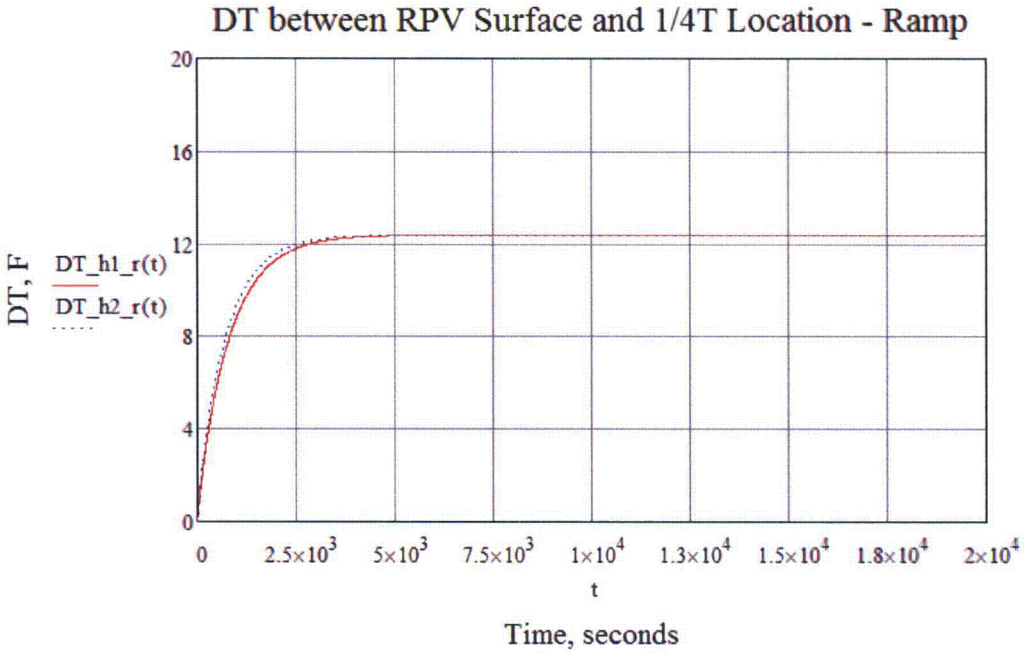

Figure 4: Temperature difference between the ID and 1/4t locations for 6 inch thick Carbon Steel Plate for a ID convection coefficient of 500 and 1000 BTU/hr-ft^2-°F, OD insulated, 100 °F/hr cool-down transient.

RAI-2

It is stated in Section 2.3.3 of the LTR that, "[t]herefore, pipe reaction loads are evaluated in order to assess the effect of piping loads on the stress intensity factor [K_I] calculated at the instrument nozzle." In the finite element method (FEM) model such as that in Figure 4-1, only the reactor pressure vessel (RPV) and the instrument nozzle are modeled. Please confirm that the "piping loads" are from the piping attached to the safe-end of the instrument nozzle only and not from the various large piping (not shown in Figure 4-1) attached to the RPV.

RAI-2 Response

Correct, the "pipe reaction loads" are from the instrument nozzle attached piping.

RAI-3

It is stated in Section 2.4 of the LTR that, "[a] stress path, with the orientation shown in Figure 2-1, is chosen for extracting hoop stress results from the FEA [finite element analysis]." Please demonstrate that selecting the 45° line as the stress path to represent the opening stresses of the entire postulated crack face in the FEA and then using the 45° line stresses as input to the subsequent boundary integral equation/influence function (BIE/IF) solution can produce reliable, conservative results.

RAI-3 Response

EPRI NP-339, "Improved Evaluation of Nozzle Corner Cracking," [4] develops stress intensity factors for feedwater nozzles using detailed 3-D finite element analyses. As an approximation to the detailed analyses, stress intensity values "were related to the one-dimensional stress distribution through the centerline of the crack." The centerline of the crack is shown as 45° in Figure 72 of Reference [4]. Good agreement between the stress intensity factors calculated from detailed analysis and the simplified one-dimensional stress distribution is shown in Figure 72 [4]. Additional work by Delvin and Riccardella [5] showed that a third order polynomial curve fit of one-dimensional stresses used to predict crack growth showed "excellent agreement with experiment, with the upper bound design curve providing a conservative but reasonable prediction of the test results." The approach in ASME 78-PVP-91 maintained the 45° angle. Recent investigations of the BIE/IF solution used in this LTR [6] have similarly used the 45° angle and concluded that it is appropriate and acceptable.

RAI-4

It is stated in Section 3.0 of the LTR regarding Assumption 3 that, "[t]herefore, applying the weaker base metal properties instead of weld material properties is typically considered conservative." Please note that by doing so, the thermal properties of the base metal might also be used in the analyses instead of the weld material thermal properties. If this is the case, please assess the impact of the difference in thermal properties on the thermal analysis results under the thermal transient shown in Figure 2-3, noting, for instance, that Table 2-3 for the base metal and table 2-5 for the assumed weld material indicate a 3 to 1 difference in their thermal conductivities.

RAI-4 Response

In Assumption 3, "base metal" is intended to mean an equivalent ASME Code material for the weld metal. There are no physical material properties in the ASME Code for as-deposited Alloy 600. Instead, physical properties for N06600 are substituted. It is not the intent of Assumption 3 to justify the use of low alloy steel properties, for example, in place of Alloy 600 properties.

Additional clarification, as identified in the underlined text below, will be added to Section 3.0, Assumption 3:

> Material properties for the weld components listed in Table 2-2 are assumed based on practices established in the ASME Boiler and Pressure Vessel (B&PV) Code, Section IX [6]. Weld material properties are based on weld procedure qualifications. Testing is the only way to verify the properties. In general, the failure location is in the base metal during material failure tests. Therefore, applying the weaker base metal properties instead of weld material properties is typically considered conservative. For example, the properties for N06600 are used in the analysis in place of the as-deposited Alloy 600 material properties.

RAI-5

It is stated in Section 4.2 that, "[t]he nodes on the free end of the safe end are coupled in the nozzle axial direction to ensure equal axial displacement of the end of the nozzle and RPV in response to the membrane load so as to simulate the effects of the attached piping and closed end of the RPV." This requires clarification. Usually, the moments and the forces from the existing piping system analysis are applied to the free end of the nozzle safe end in the FEM analysis, in addition to the membrane loads mentioned in the quote. Is the purpose of coupling to make the nozzle free end nodes move as a plane? Elaborate on why coupling the nodes on the free end of the safe end in the nozzle axial direction best simulates the real situation.

RAI-5 Response

Section 4.2 documents only a mesh sensitivity study performed to demonstrate that the spatial discretization selected for the FEMs was sufficient to resolve the parameters of interest. For this study an internal pressure load case was evaluated for which the "blow-off" load was applied to the free end of the nozzle. Consequently, the coupled boundary condition applied to the nozzle free end is correct. For the piping load cases analyzed as part of this evaluation, documented in Sections 5.3 and 6.3, the nodes at the end of the safe end are connected to a pilot node on which the appropriate forces and moments are applied.

RAI-6

It is stated in Section 6.1 that, "Figure 6-2 illustrates the circumferential stress distribution for one of the un-cracked models for the pressure load case." Since the FEM model represents a quarter of the RPV and the instrument nozzle assembly, the radial crack can be placed at any location along the 90 ° circumference of the nozzle attached end, depending on the stress values. Under the stress distribution of Figure 6-2, what is the crack plane orientation (e.g., defined by degrees from the edge of the 90 ° FEM model) which would give the highest K_Is? Discuss the effort spent in finding this critical crack plane orientation, considering that the critical crack plane orientation for the pressure load case may not be the critical crack plane orientation for the thermal load case and the critical crack plane orientations may not be the same for the 38 FEM models studied in the LTR.

RAI-6 Response

The postulated crack is always placed in an orientation such that it is normal to the maximum hoop stress in the RPV from the pressure load case. This orientation always gives the highest pressure stress intensity factor since:

1. The hoop stress is a factor of 2 larger than the axial stress in a cylindrical pressure vessel,
2. The geometric stress concentration factor caused by the nozzle penetration in the cylindrical pressure vessel is maximum at the intersection of the nozzle with the RPV along the longitudinal axis of the RPV

These two characteristics of the loading and geometry result in the bounding crack orientation always being such that the crack faces are normal to the maximum hoop stress direction.

It has been shown in References [6, 7] that the thermal stress distribution around the circumference of the nozzle blend radius does not exhibit substantial variation. Consequently, locating the postulated crack, for the thermal load case, in an orientation identical to that selected for the pressure load case results in the bounding combination of the thermal and pressure contributions to K_I, for all nozzles.

RAI-7

It is stated in Section 6.1 that, "...the stress solution exhibits a large elastic pseudo-stress adjacent to the geometric discontinuity. This pseudo-stress may be ignored since the real structure would exhibit local yielding..." Please clarify that (1) no adjustment of stresses is made as long as the pseudo-stresses are below the yield strength of the material and (2) ignoring the "pseudo-stress" means adjusting the pseudo-stress to the yield strength of the material.

RAI-7 Response

No adjustment to stress is made at any time. The entire analysis, both stress and fracture mechanics, is performed as a linear elastic analysis. The comment included in the LTR was intended only to convey that, for the purposes of the figure, the contour scale on the plot was truncated such that the peak stress in the vicinity of the discontinuity was not shown in order to more clearly illustrate the stress distribution over the remainder of the crack face, since it is this distribution which has a more significant influence on the calculated stress intensity factors for the postulated crack.

RAI-8

It is stated in Section 6.2 that, "Paths are defined for a case where the RPV clad is excluded in the path definition and for a case where the path includes the RPV clad. Figure 6-7 shows these two paths."

- *Please confirm that in both cases, the FEM model has considered RPV cladding, and the paths shown in Figure 6-7 simply represent two different paths for extracting stresses.*

- *It appears that the "Path excluding clad" shown in Figure 6-7 will pass the gap between the RPV bore and the nozzle, resulting in hoop stress discontinuity. Please confirm that this is the case in your analysis.*

- *It appears that the "Path including clad" shown in Figure 6-7 actually did not pass RPV cladding. Instead, it passes the nozzle inner end. Please confirm.*

RAI-8 Response

It is confirmed that in both cases the thermal loading was applied to the cladding and the thermo-elastic stress analysis was performed with cladding in the finite element model. Two different paths were defined to extract path stress distributions: one starting at a radial location corresponding toe the ID of the cladding, and one starting at a radial location corresponding to the ID of the LAS shell. In all cases, the path origin lies in the nozzle insert.

Neither path shown in Figure 6-7 passes through the air gap between the nozzle insert and the RPV shell.

RAI-9

The lower part of Figure 6-9 shows a plot of thermal ramp K_I for the finite element-linear elastic fracture mechanics (FE-LEFM) and the BIE/IF analyses versus the crack front location. Please explain why in the thermal case, the K_I value increases rapidly when the crack front moves from 25° to 90° while the K_I values are about the same at these two locations in the pressure case (see Figure 6-5).

RAI-9 Response

The K_I distribution along the crack front obtained from the FE LEFM evaluation provides a nodal K_I calculation. The nodal values will be influenced by the stress and strain local to each nodal position. For a load condition which does not induce a highly irregular stress distribution along the crack faces, the approximate shape of the K_I distribution along the crack front can be inferred by the stress distribution normal to the crack faces, obtained from the uncracked model. Review of the pressure load case stress distribution shows a relatively uniform stress distribution along the crack front location with some stress intensification at the hole in the reactor pressure vessel (RPV), as shown in Figures 4-6 and 6-2. Consequently, the K distribution will be relatively flat along the crack front with a small shift upward toward the free surface at the shell penetration, because of the local stress intensification. This trend is observable in Figure 4-8, where increased mesh refinement shows a local increase in the nodal K_I values near the hole in the RPV.

For the thermal load case, the thermal stresses are higher near the RPV ID; consequently, the nodal K_I values increase near the ID.

RAI-10

It is stated in Section 7.0 that, "[t]he BIE/IF solution is shown to not bound the maximum KI along the crack front obtained from the FE LEFM analysis.... For P-T curve analysis, a conservative ¼ thickness flaw is assumed; a real flaw does not exist. Consequently, the inherent conservatism in assuming a ¼ thickness flaw is considered sufficient such that requiring use of the maximum KI along the entire crack front is considered to be excessively conservative." Since a real ¼ thickness flaw does not exist for almost all plants, applying the P-T limits methodology based on this assumption is equivalent to upholding the same level of margin of fracture toughness versus the applied KI for all beltline materials, including the

instrument nozzle material, of all plants. Using the maximum applied KI along the crack front in the P-T limit analysis for the instrument nozzle is technically correct and maintains the same margin for the RPV materials of all plants. Please assess the practicality of applying a factor of 1.1 to the applied pressure KI values based on the BIE/IF and 1.4 to the applied thermal KI values based on the BIE/IF to bound the applied KI values and address (1) whether these factors will always make the instrument nozzle limiting for the P-T limit curves and (2) whether plant operation will be severely limited if the instrument nozzle becomes limiting.

RAI-10 Response

Regarding the assertion that use of the maximum applied K_I along the crack front for P-T limit analysis is technically correct it is important to revisit the intent of ASME XI Appendix G methods. The basis for the Code rules contained in ASME XI, Appendix G is documented in Welding Research Council Bulletin 175 (WRCB 175) [11]. The task group members used the burgeoning concepts of fracture mechanics to develop an analytical methodology which could ensure adequate margin against non-ductile failure of the ferritic components of the primary coolant pressure boundary. One of the fundamental aspects of this fracture mechanics based approach is the use of the linear elastic fracture mechanics (LEFM) theory to simulate onset of unstable crack propagation. This simplification was used because it allows simpler fracture mechanics methods than would be required for elastic-plastic fracture mechanics (EPFM) while also including inherent conservatisms which are not specifically quantified yet increase the actual margin against unstable crack propagation above that which is calculated. Other specific and quantified conservatisms included in the ASME XI, Appendix G methods are:

1. A required factor of 1.5 or 2, depending on the operating condition,
2. A postulated flaw size of ¼ of the wall thickness which is approximately 10 times larger than that which is acceptable in the IWB-3500 acceptance tables,
3. A lower bound curve for material fracture toughness.

Actual failure of low alloy steels used in light water reactor (LWR) pressure vessels is preceded by significant stable, ductile crack extension [16]. This material behavior is not credited when the ASME XI, Appendix G methods are used. Further, significant testing performed by Oak Ridge National Laboratory (ORNL) as part of the Heavy Section Steel Technology (HSST) program sponsored by the NRC showed that the actual margins to failure of the flawed pressure vessels tested exhibited margins to failure in excess of those predicted using the ASME XI, Appendix G methods. This additional margin is expected based on the inherent conservatisms and simplifications of the ASME XI, Appendix G methods, as discussed above. These methods have historically calculated the K_I at the "deepest" point of the postulated semi-elliptical flaw. Consistent with this practice the LEFM solution used for the current evaluation, and historically used for nozzle corner cracking, provides a K_I using path stresses taken along a path passing through the deepest point of the postulated quarter circular flaw, along the direction of the path. ASME XI, Appendix G methods have always omitted consideration of effects such as pressure on the crack face, near surface effects such as the differential thermal expansion of the clad at the clad/LAS interface, near surface perturbations to stress intensity factors caused by local stress gradients, and welding residual stresses. These simplifications are enabled because of the large conservatism both quantified and un-quantified in the ASME XI, Appendix G methodology. Flaw evaluations of in-service detected indications, in other words, evaluations of actual flaws, are performed using the methods in ASME XI, Appendix A,

which does require consideration of these effects, as well as calculation of crack growth and consideration of the K_I at the deepest point and at the surface. This increased analytical detail is required because the conservatism of the large postulated flaw is not present for an actual flaw.

It is further recognized that testing of corner cracked nozzles, performed under the HSST program, showed that failure of corner cracked nozzle specimens exhibited fracture toughness in excess of the plane strain fracture toughness; the investigators acknowledged that the specimen behavior exhibited an elevated toughness as would be characteristic of reduced constraint of the specimen at the flaw location [16]. It is known that the plane stress fracture toughness is greater than the plane strain fracture toughness [17]. Near the free surfaces the behavior of the material will be better characterized by the plane stress fracture toughness than by the plane strain value. Analytical and experimental evidence show that the elevation in fracture toughness can be substantial. Further, the extent of material expected to be influenced by the near surface reduction in constraint can be estimated by the size of the plane stress plastic zone or size of the shear lips at failure [18]. Although there are slightly different equations given by various researchers, an estimate of this size can be given by:

$$0.4 \cdot \left(\frac{K_{IC}}{\sigma_Y} \right)^2 = 0.4 \cdot \left(\frac{200}{50} \right)^2 = 6.4 \; in.$$

Although this value appears large it is essentially consistent with the fracture toughness size requirements for K_{IC} testing which show that very large specimen sizes are required before a true plane strain condition is ensured at the flaw.

Returning to the FE LEFM evaluation documented in the LTR it is acknowledged that the K_I for a single node along the crack front exceeded that K_I calculated using the BIE/IF solution for the thermal load case alone. This node is at the free surface. Based on the element sizing used in the FEA, the extent of material for which the FE based K_I is observed to be greater than the BIE/IF K_I is ~0.15 inches. This material is well within the extent of material for which the plane stress fracture toughness is more applicable.

It should also be noted that the FE LEFM K_I values along the entire crack front are everywhere bounded by the value given by the BIE/IF solution for the pressure load case. The ratio between the peak FE LEFM K_I and the BIE/IF K_I is approximately 77/62=1.24. In other words the BIE/IF based K_I for the pressure load case is 24% conservative with respect to the peak K_I along the crack front. Recognizing that ASME XI, Appendix G requires a structural factor of 2.0 to be applied to the K_I for the pressure load case and structural factor of 1.0 to be applied to the structural factor for the thermal load case, it is apparent that the pressure term dominates the calculate of the P-T limits over most of the applied pressure range. The further amplification of the already conservative pressure term adds further conservatism to the methodology selected for this LTR.

Considering that:

1. Use of near surface K_I values, rather than the deepest point is not consistent with ASME G methods, as well as,
2. The observation that near a free surface the failure is governed more appropriately by a fracture toughness elevated above the plane strain fracture toughness, which implies greater margin to failure at this location, and,
3. The pressure term, which is shown to be 24% conservative compared to the peak FE LEFM K_I is further amplified by the Code required structural factor of 2.0 compared to the Code required structural factor of 1.0 for thermal loads,

The observation that a single nodal K_I, near the free surface, from the FE LEFM analysis falls above the conservative BIE/IF solution does not represent a reduction in margin required by the ASME XI, Appendix G methods. A more appropriate comparison, consistent with the intent of ASME XI, Appendix G, is as given in Table 7-1 where the BIE is observed to be conservative by ~40% for both pressure and thermal conditions.

Regarding sub-question (1) "whether these factors will always make the instrument nozzle limiting for the P-T limit curves." This is unknown. The limiting location is determined by both applied stress intensity factor K_I (a function of applied stress and geometry) and also by the properties of the limiting plate and weld in a given vessel. It is expected that a plant specific evaluation would be required to determine whether using such factors would make the instrument nozzle always limiting for PT limits.

Regarding sub-question (2) "whether plant operation will be severely limited if the instrument nozzle becomes limiting.": As with the response to (1) above, we believe that determining the extent to which plant operation will be limited if the instrument nozzle becomes limiting due to the application of such factors will require plant specific evaluation.

However, we do not believe that the application of factors, as identified in the RAI, is warranted.

We also consider that use of the BIE/IF solution has been previously approved, without amplification. Use of a K_I solution for nozzles which provides a single-point, root mean square (RMS) determination of the K_I along a quarter-circular nozzle crack has been previously approved by the NRC, as documented in the NRC safety evaluation reports (SERs) for the following evaluations:

1. The BWROG P-T curve LTR, Rev. 0 [8],
2. Various plant specific P-T curve submittals of which Reference [9] is an example, and,
3. The General Electric generic feedwater nozzle analyses performed to resolve the rapid thermal cycling induced cracking in Boiling Water Reactor (BWR) feedwater and Control Rod Drive (CRD) nozzles [3].

These references are not intended to be an exhaustive list of the evaluations for which a single-point RMS K_I solution has been accepted for use in evaluating nozzle cracking. Rather, they are provided as examples of the analyses and applications for which this type of solution and this specific solution have been previously accepted.

Further, as documented in 10CFR50.55a [10], the NRC has accepted, without exception, ASME XI, Appendix G, which recommends the use of the nozzle corner crack solution contained in Welding Research Council Bulletin (WRCB) 175 [11]. This solution is based on a finite element analysis (FEA) documented in a paper by Gilman and Rashid [12] and augmented by experimental data collected from epoxy models. Gilman and Rashid [12] identify in the conference publication describing their FEA that the methodology they utilized provides a single point K_I estimate which is representative of an average K_I along the crack front. The K_I solution utilized in this LTR is the same type of solution in that it provides a root mean square (RMS) K_I estimate.

It is also noted that the NRC and Oak Ridge National Laboratory have independently evaluated the adequacy of the solution used in the current LTR and have published the results of their independent evaluation in Reference [6], which includes the recommendation that this solution be used for development of P-T limit curves for nozzles. The nozzle solution was also, separately evaluated at different times, for evaluation of BWR feedwater nozzle cracking [3, 5], and in support of inclusion of this solution in ASME XI, Appendix G [6, 13, 14, 15]. The authors of all of these studies conclude that use of the Boundary Integral Equation / Influence Function (BIE/IF) solution for simulation of the ¼ thickness quarter circular nozzle corner crack is acceptable.

Both the use of a single point K_I solution representative of an average or an RMS K_I value along the crack front and the specific use of the solutions included in the present LTR are considered to have been extensively validated by the industry as documented in References [3, 4, 5, 6, 12, 13, 14, 15] and reviewed and accepted by the NRC in the past as documented in References [3, 8, 9, 10]. Consequently, the use of K_I obtained from the BIE/IF solutions contained in the LTR is justified without additional factors.

RAI-11

Section 8.0 proposed generic equations for estimating applied KI due to pressure (Equation 8-1) and applied KI due to 100 °F/hr thermal ramp load (Equation 8-2). These equations are based on best-estimate linear fit of calculated results for a variety of instrument nozzles. Using the best-estimate fit will allow approximately half of the number of instrument nozzles having safety margins less than that required by 10 CFR part 50 Appendix G. The bounding line, instead of the best-estimate line, may be more appropriate. Therefore, another factor of 1.1 may be needed. After combining this factor with the factors mentioned in RAI-10 to account for the maximum applied KI along the crack front, we have a combined factor of 1.5 for the applied pressure KI values based on the BIE/IF and 1.2 to the applied thermal KI values based on the BIE/IF. Please address (1) whether these combined factors will always make the instrument nozzle limiting for the P-T limit curves and (2) whether these combined factors will alter your response to RAI-10 regarding plant operation due to instrument nozzle being limiting.

RAI-11 Response

Our responses to sub-questions (1) and (2) are the same as for RAI 10.

Regarding sub-question (1) "whether these factors will always make the instrument nozzle limiting for the P-T limit curves : This is unknown. The limiting location is determined by both applied stress intensity factor KI (a function of applied stress and geometry) and also by the properties of the limiting plate and weld in a given vessel. It is expected that a plant specific evaluation would be required to determine whether using such factors would make the instrument nozzle always limiting for PT limits.

Regarding sub-question (2) "whether plant operation will be severely limited if the instrument nozzle becomes limiting.": As with the response to (1) above, we believe that determining the extent to which plant operation will be limited if the instrument nozzle becomes limiting due to the application of such factors will require plant specific evaluation.

However, we do not believe that the application of factors as identified in the RAI is warranted.

Currently, ASME XI, Appendix G refers to the nozzle corner crack solution contained in WRCB 175 [11] for evaluation of the pressure loading on a postulated nozzle corner crack. This solution provides an average K_I along the crack front [12]. This methodology, and similar methodologies which determine a RMS K_I along the crack front, such as that used for the present LTR, have been extensively used for development of P-T limits and have been accepted for use by the NRC, as documented in the response to RAI-10 above. The FEA performed in support of the present LTR shows that the BIE/IF solution selected for the LTR provides RMS K_I values which are on the order of 40% conservative with respect to the more accurate finite element LEFM evaluations performed to benchmark adequacy of the BIE/IF solution. Since the BIE/IF solution is already shown to be conservative, with respect to the RMS K_I value, already considered to have been accepted as a parameter for use in development of P-T limits, it was considered unnecessary to add additional conservatism such that an upper bound curve fit equation was determined. As shown in the three plant specific benchmark cases, provided to demonstrate adequacy of this method, the maximum difference between the plant specific RMS K_I determined using the BIE/IF solution and the RMS K_I calculated using the curve fit equation suggested in this LTR was less than 6%. Considering that the BIE/IF solution was shown to be conservative with respect to a plant specific FEA, by 46% for the thermal ramp load case and 39% for the internal pressure load case, in this same LTR, it is not considered necessary to add further conservatism to this methodology. Consequently, we believe that keeping the curve fit equations as best-estimate curve fits rather than upper bound curve fit equations is justified.

References:

1. BWRVIP-49-A: BWR Vessel and Internals Project, Instrument Penetration Inspection and Flaw Evaluation Guidelines, EPRI, Palo Alto, CA: 2002. 1006602.
2. McNeill, D. R., Brock, J. E., *Engineering Data File, Charts for Transient Temperatures in Pipes*, Heating/Piping/Air Conditioning, pp. 107-119, November 1971.

3. Boiling Water Reactor Feedwater Nozzle/Sparger Final Report, NEDO-21821-A, February 1980, General Electric Company.
4. Cohen L. M., et. al, and Besuner, P. M., "Improved Evaluation of Nozzle Corner Cracking," EPRI NP-339, March 1977, EPRI.
5. Delvin, S. A., and P. C. Riccardella, "Fracture Mechanics Analysis of JAERI Model Pressure Vessel Test," ASME, 78-PVP-91, New York, April 5, 1978 (originally presented at the joint ASME/CSME Pressure Vessels and Piping Conference, Montreal, Canada, June 25-30, 1978), SI File No. 1000720.206.
6. Yin, S., Bass, B. R. and Stevens, G. L., December 2010, "Stress and Fracture Mechanics Analyses of Boiling Water Reactor and Pressurized Water Reactor Pressure Vessel Nozzles," Oak Ridge National Laboratory Technical Report No. ORNL/TM-2010/246, NRC ADAMS Accession No. ML110060164.
7. BWRVIP-108NP: BWR Vessel and Internals Project, Technical Basis for the Reduction of Inspection Requirements for the Boiling Water Reactor Nozzle-to-Vessel Shell Welds and Nozzle Blend Radii. EPRI, Palo Alto, CA: 2007. 1016123.
8. Stevens, G.L., "Pressure-Temperature Limits Report Methodology for Boiling Water Reactors," SIR-05-044-A, April 2007.
9. JAMES A. FITZPATRICK NUCLEAR POWER PLANT -ISSUANCE OF AMENDMENT RE: RELOCATION OF PRESSURE AND TEMPERATURE CURVES TO THE PRESSURE AND TEMPERATURE LIMITS REPORT CONSISTENT WITH TSTF-419-A (TAC NO. MD8556), ML082630365.
10. Title 10 Code of Federal Regulations Part 50.55a, Codes and Standards.
11. PVRC Ad Hoc Group on Toughness Requirements, August 1972, "PVRC Recommendations on Toughness Requirements for Ferritic Materials," WRC Bulletin No. 175, Welding Research Council, New York.
12. Gilman, J. D. and Rashid, Y. R., September 1977, "Three-Dimensional Analysis of Reactor Pressure Vessel Nozzles," Proceedings of 1st International Conference on Structural Mechanics in Reactor Technology, Volume 4, Paper G2/6.
13. Mehta, H. S., Griesbach, T. J. and Stevens, G. L., 2008, "Suggested Improvements to Appendix G of ASME Section XI Code," Proceedings of the ASME 2008 Pressure Vessels & Piping Division Conference, ASME PVP2008-61624.
14. Mehta, H.S., Griesbach, T. J., Sommerville, D. V., Stevens, G. L., "Additional Improvements to Appendix G of ASME Section XI Code for Nozzles," Proceedings of the ASME 2011 Pressure Vessels & Piping Division Conference, ASME PVP2011-57015.
15. Sommerville, D., Qin, M., Houston, E., 2011, "An Investigation of the Adequacy of a Simplified Boundary Element Integral / Influence Function Equation Linear Elastic Fracture Mechanics Solution for Nozzle Corner Cracking with Respect to ASME XI,

Appendix G," Proceedings of the ASME 2011 Pressure Vessels & Piping Division Conference, ASME PVP2011-57742.

16. Merkle, J. G., et. al., *Test of 6-in.-Thick Pressure Vessels. Series 4: Intermediate Test Vessels V-5 and V-9 with Inside Nozzle Corner Cracks*, ORNL/NUREG-7, August 1977.

17. Barsom, J. M., Rolfe, S. T., "Fracture and Fatigue Control in Structures," 3rd Ed., ASTM. 1999.

18. Lai, Man-On, The Relationship between Fracture Toughness and Shear Lip Size, Doctoral Thesis, University of Auckland, 1977.